Letter

Holographic Resonant Laser Printing of Metasurfaces Using Plasmonic Template

Marcus S. Carstensen,[†,∥] Xiaolong Zhu,[†,∥] Oseze Esther Iyore,[†] N. Asger Mortensen,[‡] Uriel Levy,[†,§] and Anders Kristensen*,[†]

†DTU Nanotech, Department of Micro and Nanotechnology, Technical University of Denmark, DK-2800 Kongens Lyngby, Denmark

‡Center for Nano Optics & Danish Institute for Advanced Study, University of Southern Denmark, Campusvej 55, DK-5230 Odense M, Denmark

§Department of Applied Physics, The Benin School of Engineering and Computer Science, The Center for Nanoscience and Nanotechnology, The Hebrew University of Jerusalem, Jerusalem, 91904, Israel

S *Supporting Information*

ABSTRACT: Laser printing with a spatial light modulator (SLM) has several advantages over conventional raster-writing and dot-matrix display (DMD) writing: multiple pixel exposure, high power endurance and existing software for computer generated holograms. We present a technique for the design and manufacturing of plasmonic metasurfaces based on ultrafast laser printing with an SLM. As a proof of principle, we have used this technique to laser print a plasmonic metalens as well as high resolution plasmonic color decorations. The high throughput holographic resonant laser printing approach enables on-demand mass-production of customized metasurfaces.

KEYWORDS: *metasurfaces, plasmonics, nanoimprint, laser printing, spatial light modulator, flat optics*
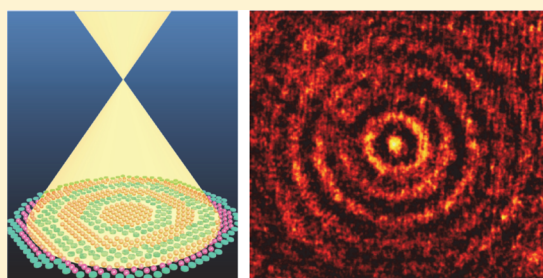
The emerging *Internet of Things*[1] stimulates the development of new sensor technology, which requires cost-efficient, compact, and lightweight optical components. Such ultrathin optical elements, of thickness comparable to the wavelength of light and even below, are achievable with optical metasurfaces:[2−20] Lithographically defined, spatially varying arrays of subwavelength dielectric or metallic elements that can control the propagation of electromagnetic radiation. In particular, metasurfaces have the capability of manipulating the phase, amplitude, and polarization of light. Recent research reports on metallic as well as dielectric or hybrid metasurfaces with diffraction-limited focusing, subwavelength resolution imaging, and for total control of reflected or transmitted light. In this paper, we present a flexible and up-scalable method for laser printing of flat optical components in prefabricated metasurfaces, extending the concepts of plasmonic colors[21−25] and ink-free color laser printing in metallic (plasmonic)[26,27] and dielectric metasurfaces,[28] which can be manufactured by production-grade methods[29] and laser reshaping and even ablation[30−35] to provide control over plasmonic colors.

In our previous work[26,28] on resonant laser printing (RLP) we obtained a world record laser printing resolution beyond 127000 DPI by raster scanning a focused laser beam across the metasurface to reshape a single nanoscale metasurface element, or unit cell, at a time. As a new paradigm, holographic laser postprocessing at the unit cell level is hereby introduced and used to inscribe local metasurface functionalities, that is, beyond the control of color for, for example, high-density information storage or security marking purposes.[23] In order to advance the writing speed, the laser beam is reflected on a holographic SLM (LCOS-SLM X10468) to generate and translate multiple foci (800 × 600 pixels) and expose 128 × 128 unit cells in 100 ms. In this way, we improve writing speeds by orders of magnitude. SLMs are widely used for ultrafast 3D laser micromachining,[36] known as holographic femtosecond laser processing[37] and laser-lithography.[38] As a proof of concept for the effectivness of our approach, we demonstrate holographic resonant laser printing (HRLP) of various flat optics components such as Fresnel zone plate (FZP) lenses with nearly diffraction-limited focusing and axicons in plasmonic metasurfaces comprising a CMOS compatible approach with ultrathin aluminum (Al) films.[39,40] We also use the technique for single-exposure writing of plasmonic color images. Our results open a new avenue for manufacture of small series or individualized products by laser postprocessing of components that are volume manufactured with a common optical metasurface template. The laser postprocessing method also allows for individual alignment of optical elements on complex,

or assembled components, for example, plastic sensor chips, as well as trimming of the optical elements even at the metasurface unit-cell level.[41,42]

Taking advantage of plasmon-enhanced light−matter interactions,[43] we laser-postprocess Al metasurfaces with morphology-dependent resonances. Strong plasmonic absorption under pulsed laser irradiation locally elevates the temperature in a very short time scale (1 ns), where rapid photothermal melting/sintering of the metal allows for morphology changes[26,31,43,44] with associated spatially modification of transmittance. With the excitation of the surface plasmon resonances, the plasmon-enhanced photothermal melting ensures that the writing process only takes place at the plasmonic metasurface within the focal plane, causing a strong heat power confined at the interface and thus decreases the power consumption. To avoid the need for tedious and time-consuming scanning procedures we have developed the approach of HRLP, in which an image is being projected on a uniform array of metasurfaces. It is the spatial variation of this image, generated by an SLM and projected onto the metasurface plane, which controls the individual final shape of each and every metal disk, allowing the implementation of various flat optics devices and decoration effects.

The FZP[45−47] represents one particular class of flat, thin optical lenses, where the intensity and the phase of the transmitted light is spatially modulated by concentric ring zones to focus the light at a given distance away from the substrate. There are two classifications of FZPs, based on either amplitude or phase modulation. Clearly, one can also implement a hybrid type of FZP, where both the amplitude and the phase are spatially modulated. In all cases, the periodicity of the rings is becoming shorter toward the periphery such that the FZP supports higher diffraction angles needed for the focusing of optical rays far from the optical axis. A binary amplitude FZP, as demonstrated by Li et al.,[46] comprises a sequence of transparent and opaque, concentric ring zones. A binary phase FZP[45] can be fabricated by etching or adding the concentric ring zones of an optically transparent material, whereby the optical thickness, and thereby, the phase of the transmitted light is modulated spatially. The phase-based FZP provides higher diffraction efficiency. An adaptive FZP reported by Wang et al.[47] utilizes laser-induced heating in a phase-changing material. To define the concentric ring zones, the contrast in dielectric properties is obtained by switching between an amorphous state and multiple metastable cubic crystalline states by use of a short high-density laser pulse. Hereby, we demonstrate experimentally a laser printed ultrathin FZP within plasmonic metasurfaces. Figure 1a shows a schematic of a transmissive plasmonic FZP fabricated by RLP. The building elements of the ultrathin FZP are prefabricated plasmonic nanoresonators, which are subsequently laser reconfigured. Space-variant metasurfaces can be constructed from plasmonic resonators either for focusing, Figure 1b, or for other types of beam manipulations, for example, the construction of axicons which are typically used to form nondiffractive Bessel beams, Figure 1c. The HRLP technology is employed to spatially modify the transmittance of the plasmonic metasurfaces. In contrast to many previous designs, our FZP is only 50 nm (approximately one-tenth of the wavelength) thick and can potentially be mass-produced.

In plasmon-assisted laser printing, pulsed-laser irradiation generates transient thermal power in the plasmonic structures which in turn modifies the spectroscopic transmission patterns
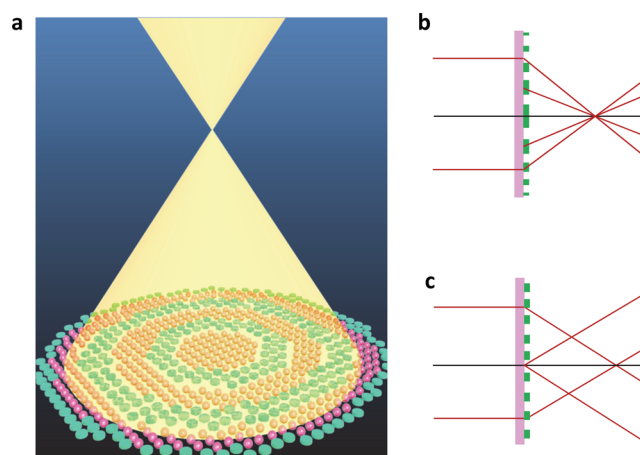

Figure 1. (a) Illustration of laser printed flat optics. (b) Schematics of a FZP and (c) an axicon lens made by an ultrathin patterned layer of plasmonic nanostructures.

by melting and reshaping the structures. As illustrated in Figure 2a, we developed a mask-free RLP technology to pattern plasmonic resonant metasurfaces with a superior resolution. This technology uses a pulsed laser (1 ns pulse duration) with an on-resonance frequency (corresponding to a wavelength of 532 nm) and related apparatus to control the intensity of the pulse trains, the 3D motion of the samples and diffraction-limited focusing of the laser spot. As a result, different plasmonic resonances arise depending on the laser pulse energy density, which in turn leads to different transmittances as well as an on-resonance phase change. The RLP technique here was extended to an HRLP technique which is developed as a flexible and single shot postwriting technology for flat optics, where rapid melting of a ~100 × 100 μm^2 area allows for surface-energy-driven morphology changes with associated modification of amplitude, phase, and polarization of the reflected, transmitted, and scattered light over each individual element of the plasmonic metasurfaces. Figure 2b shows the transmitted amplitude control of an axicon lens that is conducted by our HRLP technique.

To manipulate the strength of the transmittance we controlled intensity of optical pulses, while preserve their repetition rate, typically at 1 kHz. We achieved a diffraction limited resolution of printing using a lens with a numerical aperture (NA) of 0.85 and a magnification of 50× (Figure 2a). When applying the HRLP to a plasmonic metasurface with a resonance located at 600 nm, the resonant transmittance peak of the printed area blueshifts from 600 to 500 nm, which results in the contrast in the transmission images as in Figure 2b. The proof of concept experiments were relayed on a plasmonic metasurface formated by depositing a thin film (20 nm) of aluminum on top of an array of dielectric (OrmoComp, microresist technology GmbH, Berlin, Germany) pillars with a height of 30 nm, a radius of 45 nm and a periodicity of 200 nm. The transmittance of the printed areas was measured by an imaging spectrometer with a grating of 300 lines/mm (Andor Shamrock 303i and Newton 920 CCD camera). Results due to white-light illumination are shown in Figure 2c. Gradually tuning the laser intensity upon printing, we demonstrated the manipulation of the transmittance at a certain wavelength (e.g., 532 nm). As shown in Figure 2d, more than 2× transmission contrast between the pristine and printed samples can be achieved with laser pulses of a couple of μJs.
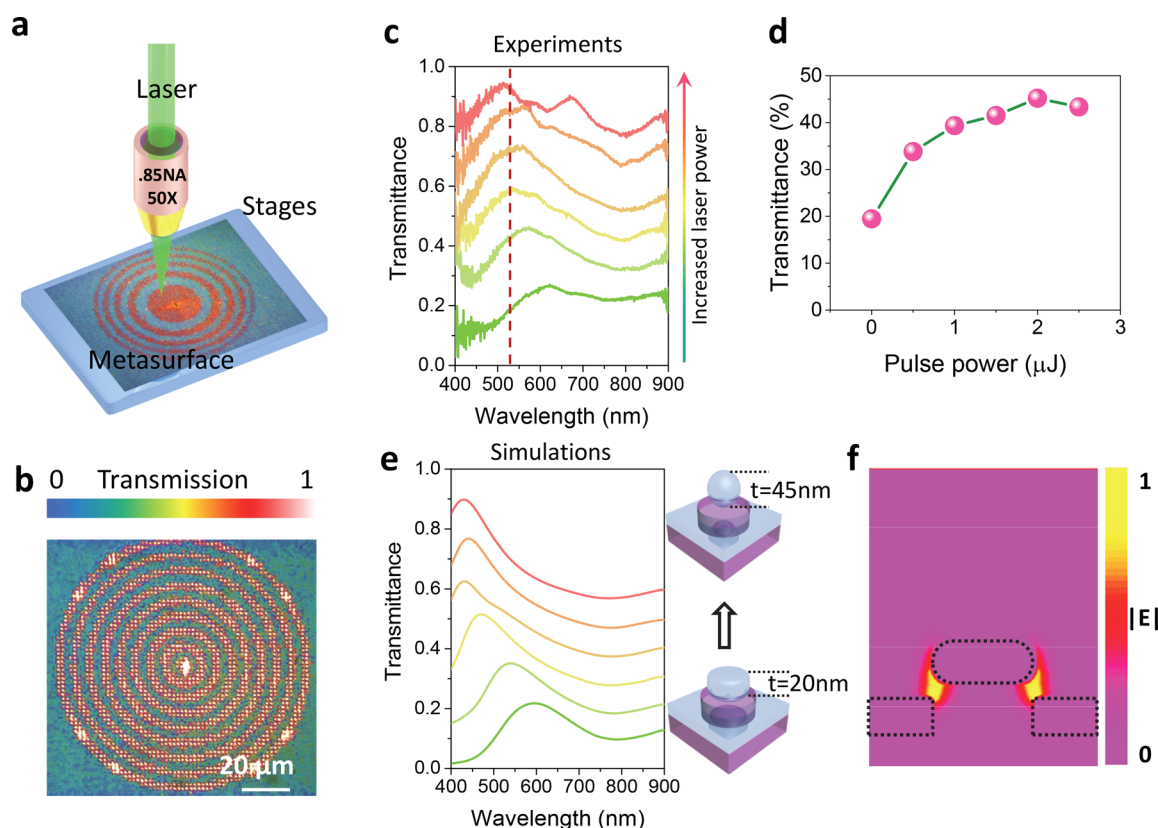
Figure 2. (a) schematic setup and laser printing of the ultrathin lens on optical metasurfaces. (b) Amplitude contrast presented by the transmission difference between the printed and nonprinted zones. The transmitted signals are normalized and taken under a white-light illumination. (c) Experimental transmittance spectra of the printed zones which are printed with different laser intensities. For clarity, the spectra have been stacked with a +0.1 displacement. (d) Corresponding absolute transmittance at the wavelength of 532 nm under different printing power which are read from (c) (indicated by the dashed red line). (e) Simulated transmittance spectra for laser modulated metasurfaces. For clarity, the spectra have been stacked with a + 0.1 displacement. (f) Normalized electric field distribution of the original plasmonic nanostructure at a 532 nm excitation.
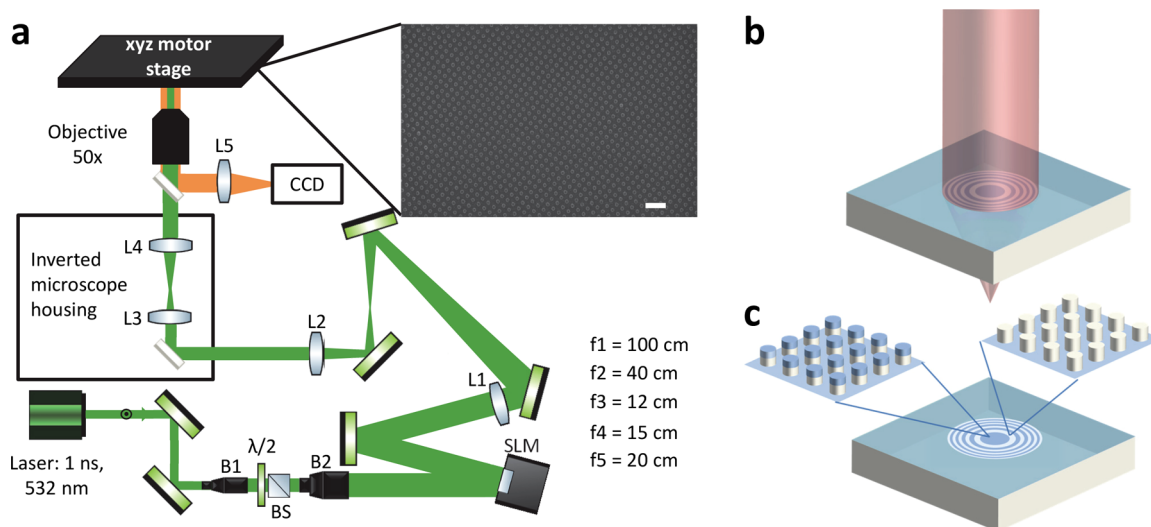

Figure 3. (a) Optical configuration for single-shot laser printing with the aid of a spatial light modulator (SLM). We used a half-wave plate and a beam splitter (BS) to continuously modulate the laser pulse energy when printing. Beam expanders (B1 and B2) were employed to match the spot size onto the SLM window. Several lenses (L1−L4) are used to generate and recover the Fourier plane at the end-surfaces, as well as to ensure full coverage of the aperture of the microscope objective. Inset shows a SEM image of a representative plasmonic metasurface. Scale bar: 500 nm. (b, c) Concept of laser printed flat optics, here illustrated by the writing of a Fresnel zone plate (FZP) in a plasmonic template.

Following previous works,[26,28] we used a simplified model of the complex thermodynamic phase transition. By sweeping the thickness (from 20 to 45 nm with a 5 nm step, as illustrated in the right of Figure 2e) of round-cornered disks (to the final

spherical shape), while preserving the overall initial material volume of the disks in simulations, the plasmonic peak varies from 600 to 450 nm (Figure 2e). For the transmittance, the result also matches the resonance induced enhanced trans-

mitted signal in Figure 2d. The substantial increasing of the transmittance at 532 nm is attributed to the fact that the melted disks together with the underneath holes support a strong hybridized plasmonic resonance.[27] The excitation of that resonance arouses the extraordinary optical transmission which is now well-known to be due to the interaction of the light with electronic resonances in the surface of the metal film,[48] as shown in Figure 2f. It should be mentioned that we used a simplified model of the complex thermodynamic phase transition. In Figure 2c, the peaks are seen in the experimental spectra for the highest laser intensities. This can be attributed to the further laser-induced modification of the structure, leading to multiple resonances as well as the extra peaks in the transmittance spectra.

Holographic resonant laser printing with an SLM has several advantages over conventional raster-writing[49] and dot-matrix display (DMD) writing: multiple pixel exposure, high power endurance and existing convenience for computer generated holograms (CGH), see also the Supporting Information. Figure 3a shows the optical setup that has been used for the HRLP. Briefly, the beam emerging from a frequency-doubled Nd:YAG laser is expanded, and its intensity is controlled via a polarized beam splitter and a half waveplate. Next, light is impinging on the SLM, and the desired hologram is being created. Finally, the image of the hologram is projected onto the back aperture plane of a microscope objective. In the focal plane of the microscope objective, a Fourier transform of the image is being created and this desired light distribution is interacting with the metasurface pattern. Figure 3b,c shows the concept of laser printed flat optics, illustrated by the writing of a Fresnel zone plate (FZP) in a plasmonic template constituted by hybridized nanodisk and nanohole arrays, initially developed for plasmonic colors,[27] and now available through mass-production techniques.[29] Because of advantages of HRLP, most of the current commercial lasers can provide the needed power even for laser printing with hi-res SLMs, for instance, the 4K SLM with 3840 × 2160 pixels (EXULUS-4K1, Thorlabs), which will highly improve the uniformity of exposed patterns.

To realize easy-to-fabricate ultrathin flat FZPs, we implemented the HRLP by an SLM providing 800 × 600 pixels, where the laser intensity is varying dynamically in space. Figure 4a shows a printed plasmonic metasurface optical component (100 μm in width) with an optimized transmission contrast serving as a focusing lens. While classic silica lenses are several millimeters thick, the plasmonic FZP features a 50 nm functional layer of Al disk-hole structures. Figure 4b shows a scanning electron microscopy (SEM) image of a part of the fabricated FZP with exposed and unexposed areas of outermost rings composed of dense plasmonic elements. Typical hologram from SLM achieves diffraction pattern in the first diffraction order. The remaining light intensity is mostly located in the zero-diffraction order, which results in the defects in HRLP. In order to avoid this zeroth peak from the SLM, one can adjust the focus positions and transform the original on-axis diffractive images into off-axis ones by combining a blazed grating or a FZP in the original CGH patterns. However, the method to spatially separate the undesired zeroth order from the first order has disadvantages, such as the geometric distortions, the beam aberrations and the decreasing of the printing energy. In this work, the original CGH is used as a proof-of-concept method for HRLP. Noted that the light transmitted from the defect consists a very small portion of the light at the focal point when considering the size.
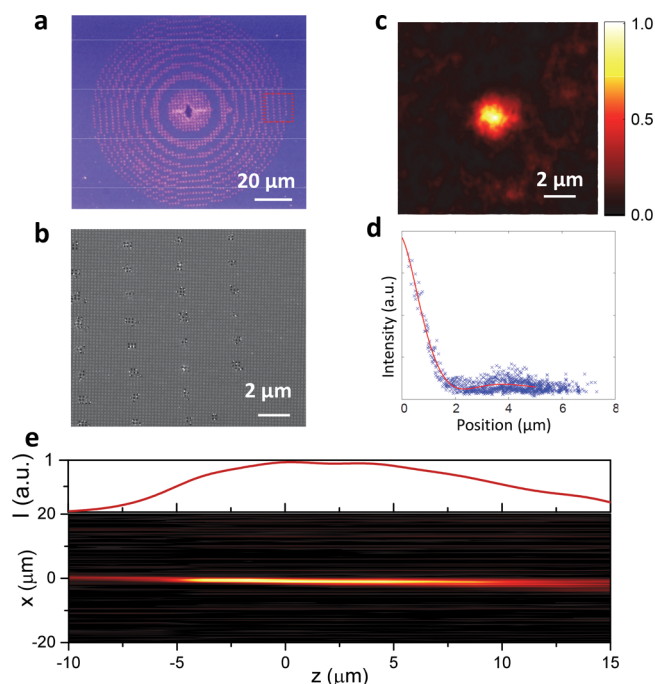
Figure 4. (a) Microscopic image of a fabricated FZP. Scale bar: 20 μm. (b) SEM image of a selected region (red box) in (a) which shows both the printed and unprinted areas. Scale bar: 2 μm. (c) Experimentally obtained image of the focused plane under a 532 nm laser illumination. (d) Fitted experimental focal field intensity for laser illumination with wavelength of 532 nm by integrating the intensity signals in a radial manner, which results in (a) . (e) Measured beam intensity profile of the FZP in the axial direction around the focal point. The intensity (I) along the center of focal beam is plotted along the z axis.

When illuminated with a coherent plane wave at a wavelength of 532 nm, the printed FZP creates a highly symmetric focal spot at a distance of 258 μm, as shown in Figure 4c. Note that the experimental focal distance is slightly shorter than the theoretical design (300 μm), which probably originates from limited fabrication precision while performing the pixelized Fourier transformation within the SLM. Figure 4d shows a diffraction-limited ($\lambda/2$ NA) full-width at half-maximum (fwhm) of about 1.5 μm by integrating the intensity signals in a radial manner of the focal spot. In addition, we also measured the beam intensity profile of the FZP in the axial direction around the focal point (Figure 4e). It should be mentioned that the long-working-distance flat lens may play a role in applications such as optofluidics[50] or optical trapping.[51]

Because of its full flexibility, large-scale capability, and direct one-step process, HRLP may revolutionize the conventional product chain for optical systems and has the potential to commercialize the integrated optoelectronic system with printed flat optics. To demonstrate the diversity of our technology and its strength for end-products, we next relax the extreme conditions of this method. Plasmonic metasurfaces made by deep-UV stepper lithography (a main-steam industrial manufacturing tool) were also fabricated and subsequently employed and HRLP-patterned with other functional flat optical components. When illuminated with a coherent plane-wave light beam at a 635 nm wavelength, laser printed metasurface optical components serving as a lens (Figure 5a, see also in the Supporting Information) and an axicon (Figure 5b) create a single focal spot (Figure 5c) and a nondiffractive Bessel beam (Figure 5d), respectively. Moreover, the laser
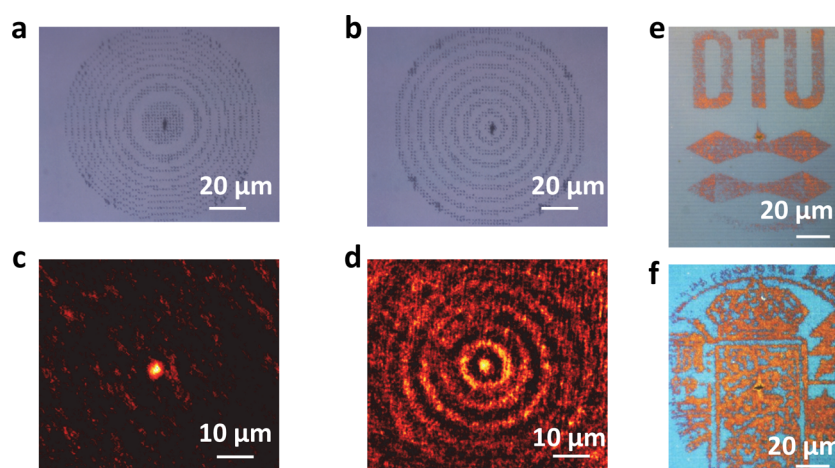
Figure 5. (a) Microscopic images of a fabricated FZP and (b) an axicon on plasmonic metasurface fabricated by DUV lithography. Scale bar: 20 μm. (c) Experimentally obtained images of the focused plane via the corresponding FZP and (d) axicon under a 635 nm laser illumination. (e, f) Graphics printed by holographic laser beam reconstructions with the SLM.

printing on plasmonic colored metasurfaces with spatial wave shaping by the SLM is also immediately applicable for more efficient plasmonic color printing. Figure 5e,f presents graphics in red printed by holographic laser beam reconstructions. It is worthy to emphasize that the results further reveal the strength of HRLP for flat optics, high definition and ink-free color printing and with a potential for future functional metasurfaces.

To sum up, as a superior alternative to using state-of-the-art and costly fabrication technologies, we demonstrate that HRLP, which is realized by applying opto-thermal modification of individual nanoscale elements, combined with holographic projection of an image pattern using an SLM, is a powerful tool for the fabrication of ultrathin flat optics within plasmonic metasurfaces. Ultrathin flat FZPs and axicons capable of generating diffraction-limited focal spots and nondiffractive Bessel beams are achieved with the HRLP process. The concept of HRLP makes the meta-optics closer to reality by providing a path for mass-production and ready-for-applications technique. This may pave the way of ultrathin flat optics into consumer products in everyday life.

ASSOCIATED CONTENT

Ⓢ Supporting Information

The Supporting Information is available free of charge on the ACS Publications website at DOI: 10.1021/acsphotonics.7b01358.

> We provide further details on the design, phase modulation pattern, and laser printing of FZP (Figure S1), as well as the measured and theoretical predicted fwhm (Figure S2) (PDF).

AUTHOR INFORMATION

Corresponding Author

*E-mail: anders.kristensen@nanotech.dtu.dk.

ORCID Ⓘ

N. Asger Mortensen: 0000-0001-7936-6264
Uriel Levy: 0000-0002-5918-1876
Anders Kristensen: 0000-0001-9567-1656

Author Contributions

‖Equal contributions by X.Z. and M.S.C.

Notes

The authors declare no competing financial interest.

REFERENCES

(1) Buyya, R., Dastjerdi, A. V., Eds. In *Internet of Things: Principles and Paradigms*, 1st ed.; Elsevier Inc.: Amsterdam, 2016.

(2) Kildishev, A. V.; Boltasseva, A.; Shalaev, V. M. Planar Photonics with Metasurfaces. *Science* **2013**, *339*, 1289.

(3) Yu, N.; Capasso, F. Flat optics with designer metasurfaces. *Nat. Mater.* **2014**, *13*, 139−150.

(4) Zhao, Y.; Liu, X.-X.; Alu, A. Recent advances on optical metasurfaces. *J. Opt.* **2014**, *16*, 123001.

(5) Yu, N.; Capasso, F. Optical Metasurfaces and Prospect of Their Applications Including Fiber Optics. *J. Lightwave Technol.* **2015**, *33*, 2344−2358.

(6) Ding, F.; Pors, A.; Bozhevolnyi, S. I. Gradient metasurfaces: a review of fundamentals and applications. *Rep. Prog. Phys.* **2018**, *81*, 026401.

(7) Hsiao, H.-H.; Chu, C. H.; Tsai, D. P. Fundamentals and Applications of Metasurfaces. *Small Methods* **2017**, *1*, 1600064.

(8) Qin, F.; Ding, L.; Zhang, L.; Monticone, F.; Chum, C. C.; Deng, J.; Mei, S.; Li, Y.; Teng, J.; Hong, M.; Zhang, S.; Alú, A.; Qiu, C.-W. Hybrid bilayer plasmonic metasurface efficiently manipulates visible light. *Sci. Adv.* **2016**, *2*, e1501168.

(9) Rogers, E. T. F.; Lindberg, J.; Roy, T.; Savo, S.; Chad, J. E.; Dennis, M. R.; Zheludev, N. I. A super-oscillatory lens optical microscope for subwavelength imaging. *Nat. Mater.* **2012**, *11*, 432−435.

(10) Arbabi, A.; Horie, Y.; Bagheri, M.; Faraon, A. Dielectric metasurfaces for complete control of phase and polarization with subwavelength spatial resolution and high transmission. *Nat. Nanotechnol.* **2015**, *10*, 937−943.

(11) Pors, A.; Albrektsen, O.; Radko, I. P.; Bozhevolnyi, S. I. Gap plasmon-based metasurfaces for total control of reflected light. *Sci. Rep.* **2013**, *3*, 2155.

(12) High, A. A.; Devlin, R. C.; Dibos, A.; Polking, M.; Wild, D. S.; Perczel, J.; de Leon, N. P.; Lukin, M. D.; Park, H. Visible-frequency hyperbolic metasurface. *Nature* **2015**, *522*, 192−196.

(13) Khorasaninejad, M.; Chen, W. T.; Devlin, R. C.; Oh, J.; Zhu, A. Y.; Capasso, F. Metalenses at visible wavelengths: Diffraction-limited focusing and subwavelength resolution imaging. *Science* **2016**, *352*, 1190−1194.

(14) Lin, D.; Fan, P.; Hasman, E.; Brongersma, M. L. Dielectric gradient metasurface optical elements. *Science* **2014**, *345*, 298−302.

(15) Chong, K. E.; Staude, I.; James, A.; Dominguez, J.; Liu, S.; Campione, S.; Subramania, G. S.; Luk, T. S.; Decker, M.; Neshev, D. N.; Brener, I.; Kivshar, Y. S. Polarization-Independent Silicon Metadevices for Efficient Optical Wavefront Control. *Nano Lett.* **2015**, *15*, 5369−5374.

(16) Guo, R.; Rusak, E.; Staude, I.; Dominguez, J.; Decker, M.; Rockstuhl, C.; Brener, I.; Neshev, D. N.; Kivshar, Y. S. Multipolar Coupling in Hybrid Metal-Dielectric Metasurfaces. *ACS Photonics* **2016**, *3*, 349−353.

(17) Bomzon, Z.; Biener, G.; Kleiner, V.; Hasman, E. Space-variant Pancharatnam-Berry phase optical elements with computer-generated subwavelength gratings. *Opt. Lett.* **2002**, *27*, 1141−1143.

(18) Levy, U.; Tsai, C.-H.; Kim, H.-C.; Fainman, Y. Design, fabrication and characterization of subwavelength computer-generated holograms for spot array generation. *Opt. Express* **2004**, *12*, 5345−5355.

(19) Levy, U.; Kim, H.-C.; Tsai, C.-H.; Fainman, Y. Near-infrared demonstration of computer-generated holograms implemented by using subwavelength gratings with space-variant orientation. *Opt. Lett.* **2005**, *30*, 2089−2091.

(20) Boroviks, S.; Deshpande, R. A.; Mortensen, N. A.; Bozhevolnyi, S. I. Multifunctional Metamirror: Polarization Splitting and Focusing. *ACS Photonics* **2018**, *5*, na.

(21) Kumar, K.; Duan, H.; Hegde, R. S.; Koh, S. C. W.; Wei, J. N.; Yang, J. K. W. Printing colour at the optical diffraction limit. *Nat. Nanotechnol.* **2012**, *7*, 557−561.

(22) Gu, Y.; Zhang, L.; Yang, J. K. W.; Yeo, S. P.; Qiu, C.-W. Color generation via subwavelength plasmonic nanostructures. *Nanoscale* **2015**, *7*, 6409−6419.

(23) Kristensen, A.; Yang, J. K. W.; Bozhevolnyi, S. I.; Link, S.; Nordlander, P.; Halas, N. J.; Mortensen, N. A. Plasmonic colour generation. *Nat. Rev. Mater.* **2016**, *2*, 16088.

(24) Hedayati, M. K.; Elbahri, M. Review of Metasurface Plasmonic Structural Color. *Plasmonics* **2017**, *12*, 1463−1479.

(25) Duan, X.; Kamin, S.; Liu, N. Dynamic plasmonic colour display. *Nat. Commun.* **2017**, *8*, 14606.

(26) Zhu, X.; Vannahme, C.; Højlund-Nielsen, E.; Mortensen, N. A.; Kristensen, A. Plasmonic colour laser printing. *Nat. Nanotechnol.* **2015**, *11*, 325−329.

(27) Clausen, J. S.; Højlund-Nielsen, E.; Christiansen, A. B.; Yazdi, S.; Grajower, M.; Taha, H.; Levy, U.; Kristensen, A.; Mortensen, N. A. Plasmonic Metasurfaces for Coloration of Plastic Consumer Products. *Nano Lett.* **2014**, *14*, 4499−4504.

(28) Zhu, X.; Yan, W.; Levy, U.; Mortensen, N. A.; Kristensen, A. Resonant-laser-printing of structural colors on high-index dielectric metasurfaces. *Sci. Adv.* **2017**, *3*, e1602487.

(29) Højlund-Nielsen, E.; Clausen, J. S.; Mäkela, T.; Thamdrup, L. H.; Zalkovskij, M.; Nielsen, T.; Li Pira, N.; Ahopelto, J.; Mortensen, N. A.; Kristensen, A. Plasmonic Colors: Toward Mass Production of Metasurfaces. *Adv. Mater. Technol.* **2016**, *1*, 1600054.

(30) Kuznetsov, A. I.; Evlyukhin, A. B.; Gonçalves, M. R.; Reinhardt, C.; Koroleva, A.; Arnedillo, M. L.; Kiyan, R.; Marti, O.; Chichkov, B. N. Laser Fabrication of Large-Scale Nanoparticle Arrays for Sensing Applications. *ACS Nano* **2011**, *5*, 4843−4849.

(31) Zijlstra, P.; Chon, J. W. M.; Gu, M. Five-dimensional optical recording mediated by surface plasmons in gold nanorods. *Nature* **2009**, *459*, 410−413.

(32) Zhu, X.; Hedayati, M. K.; Raza, S.; Levy, U.; Mortensen, N. A.; Kristensen, A. Digital resonant laser printing: Bridging nanophotonic science and consumer products. *Nano Today* **2018**, *18*, na.

(33) Makarov, S. V.; Zalogina, A. S.; Tajik, M.; Zuev, D. A.; Rybin, M. V.; Kuchmizhak, A. A.; Juodkazis, S.; Kivshar, Y. Light-Induced Tuning and Reconfiguration of Nanophotonic Structures. *Laser Photon. Rev.* **2017**, *11*, 1700108.

(34) González-Rubio, G.; Díaz-Núñez, P.; Rivera, A.; Prada, A.; Tardajos, G.; González-Izquierdo, J.; Bañares, L.; Llombart, P.; Macdowell, L. G.; Alcolea Palafox, M.; Liz-Marzán, L. M.; Peña-Rodríguez, O.; Guerrero-Martínez, A. Femtosecond laser reshaping yields gold nanorods with ultranarrow surface plasmon resonances. *Science* **2017**, *358*, 640−644.

(35) Zuev, D. A.; Makarov, S. V.; Mukhin, I. S.; Milichko, V. A.; Starikov, S. V.; Morozov, I. A.; Shishkin, I. I.; Krasnok, A. E.; Belov, P. A. Fabrication of Hybrid Nanostructures via Nanoscale Laser-Induced Reshaping for Advanced Light Manipulation. *Adv. Mater.* **2016**, *28*, 3087−3093.

(36) Malinauskas, M.; Zukauskas, A.; Hasegawa, S.; Hayasaki, Y.; Mizeikis, V.; Buividas, R.; Juodkazis, S. Ultrafast laser processing of materials: from science to industry. *Light: Sci. Appl.* **2016**, *5*, e16133.

(37) Hasegawa, S.; Hayasaki, Y. Holographic Vector Wave Femtosecond Laser Processing. *Int. J. Optomechatronics* **2014**, *8*, 73−88.

(38) Vizsnyiczai, G.; Kelemen, L.; Ormos, P. Holographic multi-focus 3D two-photon polymerization with real-time calculated holograms. *Opt. Express* **2014**, *22*, 24217−24223.

(39) Knight, M. W.; King, N. S.; Liu, L.; Everitt, H. O.; Nordlander, P.; Halas, N. J. Aluminum for Plasmonics. *ACS Nano* **2014**, *8*, 834−840.

(40) Gérard, D.; Gray, S. K. Aluminium plasmonics. *J. Phys. D: Appl. Phys.* **2015**, *48*, 184001.

(41) Zuev, D. A.; Makarov, S. V.; Mukhin, I. S.; Milichko, V. A.; Starikov, S. V.; Morozov, I. A.; Shishkin, I. I.; Krasnok, A. E.; Belov, P. A. Fabrication of Hybrid Nanostructures via Nanoscale Laser-Induced Reshaping for Advanced Light Manipulation. *Adv. Mater.* **2016**, *28*, 3087−3093.

(42) Lepeshov, S.; Krasnok, A.; Muldhin, I.; Zuev, D.; Gudovskikh, A.; Milichko, V.; Belov, P.; Miroshnichenko, A. Fine-Tuning of the Magnetic Fano Resonance in Hybrid Oligomers via fs-Laser-Induced Reshaping. *ACS Photonics* **2017**, *4*, 536−543.

(43) Chen, X.; Chen, Y.; Yan, M.; Qiu, M. Nanosecond Photothermal Effects in Plasmonic Nanostructures. *ACS Nano* **2012**, *6*, 2550−2557.

(44) Novikov, S. M.; Frydendahl, C.; Beermann, J.; Zenin, V. A.; Stenger, N.; Coello, V.; Mortensen, N. A.; Bozhevolnyi, S. I. White Light Generation and Anisotropic Damage in Gold Films near Percolation Threshold. *ACS Photonics* **2017**, *4*, 1207−1215.

(45) Rastani, K.; Marrakchi, A.; Habiby, S. F.; Hubbard, W. M.; Gilchrist, H.; Nahory, R. E. Binary phase Fresnel lenses for generation of two-dimensional beam arrays. *Appl. Opt.* **1991**, *30*, 1347−1354.

(46) Li, X.; Wei, L.; Poelma, R. H.; Vollebregt, S.; Wei, J.; Urbach, H. P.; Sarro, P. M.; Zhang, G. Q. Stretchable Binary Fresnel Lens for Focus Tuning. *Sci. Rep.* **2016**, *6*, 25348.

(47) Wang, Q.; Rogers, E. T. F.; Gholipour, B.; Wang, C.-M.; Yuan, G.; Teng, J.; Zheludev, N. I. Optically reconfigurable metasurfaces and photonic devices based on phase change materials. *Nat. Photonics* **2016**, *10*, 60−65.

(48) Genet, C.; Ebbesen, T. W. Light in tiny holes. *Nature* **2007**, *445*, 39−46.

(49) Chen, H.; Bhuiya, A. M.; Ding, Q.; Johnson, H. T.; Toussaint, K. C., Jr Towards do-it-yourself planar optical components using plasmon-assisted etching. *Nat. Commun.* **2016**, *7*, 10468.

(50) Psaltis, D.; Quake, S. R.; Yang, C. Developing optofluidic technology through the fusion of microfluidics and optics. *Nature* **2006**, *442*, 381−386.

(51) Woerdemann, M.; Alpmann, C.; Esseling, M.; Denz, C. Advanced optical trapping by complex beam shaping. *Laser Phot. Rev.* **2013**, *7*, 839−854.